Iranian Journal of Chemical Engineering
Vol. 6, No. 1 (Winter), 2009, IAChE

Research note

Unsteady-State Modeling of the Fluidized Bed Polyethylene Reactor

A. Hassimi, N. Mostoufi[*]*, R. Sotudeh-Gharebagh*

Process Design and Simulation Research Center, Department of Chemical Engineering, University of Tehran, Iran.

Abstract

A mathematical model is developed for describing the dynamic behavior of the gas phase ethylene polymerization reactor. The model is based on the dynamic two-phase concept of fluidization in which the bubbles may contain solid particles and the emulsion is capable of containing more gas than that of minimum fluidization. The fluidized bed reactor is divided into several serial sections consisting of bubble and emulsion phases. Flow of the gas is considered as plug flow through the bubbles and perfectly mixed through the emulsion phase. Polymerization reactions occur in both emulsion and bubble phases. Variation of the process variables as well as the polymer properties were studied as a function of operating time. The bed height was controlled by the product withdrawal rate with a PID controller. The results of the model were compared with the experimental data and a good agreement was observed between the model prediction and actual data. The simulation results indicate that a significant amount of polymer production (roughly 12%) takes place in the bubbles.

Keywords: *Fluidization, Polyethylene, Dynamic simulation,Gas-phase polymerization*

1. Introduction

Gas-phase catalytic fluidized-bed reactors have been widely used as one of the main methods for producing polyolefines. Production of linear low density polyethylene (LLDPE) in a gas-phase reactor using Zeigler-Natta catalyst is one of such processes. Understanding the dynamic behavior of this reactor is critical, especially in the start-up and shut-down of the reactor as well as in the grade transition process. There are various models for the dynamic behavior of the reactor and polymer properties. Choi and Ray [1] were the first to consider both emulsion and bubble phases in modeling the polyethylene fluidized bed reactor. They assumed constant bubble size along the bed and controlled the reactor temperature with a PID controller under feedback control. McAuley et al. [2] considered the polymerization reactor as a well-mixed reactor to develop the kinetic model. McAuley et al. [3] compared the two-phase and well mixed models. They showed that the simple well mixed model does not introduce significant error as compared to that of a two-phase model.

Fernandes and Lona [4,5] modeled the

∗ Corresponding author: E-mail: mostoufi@ut.ac.ir

reactor by a heterogeneous three-phase model (emulsion gas, emulsion polymer particles and bubble). Hatzantonis et al. [6] considered the effect of the varying bubble size with respect to the bed height in their model. They divided the reactor into two sections: emulsion phase in a single plug flow reactor (PFR) and bubble phase in *N* serial well mixed reactors. Chatzidoukas et al. [7] approximated the reactor behavior by a single-phase continuous stirred tank reactor (CSTR) to study the optimal grade transition procedure. They considered the necessary feedback and feedforward control loops and determined the optimal control pairings between manipulated and controlled variables of the reactor employing the complicated mathematical methods.

Alizadeh et al. [8] considered the gas-phase polyethylene reactor as three pseudo-homogeneous reactors assuming a mean voidage for the bed. They employed a tanks-in-series model to represent the hydro-dynamics of the reactor. Kiashemshaki et al. [9] developed a two-phase model for the polyethylene reactor based on the hydrodynamic model of Jafari et al. [10]. In their model, the reactor was divided into four serial sections, each section consisting of bubble and emulsion phases. Although in all of these models it was assumed that the polymerization reactions take place only in the emulsion phase, Kiashemshaki et al. [9] considered that polymerization reactions simultaneously occur in both emulsion and bubble phases, according to the dynamic two-phase concept of fluidization [11].

Kiashemshaki et al. [9] showed that the amount of polymer produced inside the bubbles is not negligible. In the present work, a dynamic model is proposed for estimating the behavior of the gas-phase ethylene polymerization reactor based on the steady-state model of Kiashemshaki et al. [9]. Adding a proper level controller to the model, it was then employed for investigating the start-up of the reactor. Unlike other dynamic models, existence of the polymer particles in the bubble phase is considered. A more realistic dynamic model results in a better understanding of the behavior of the reactor during grade transition, start up and shut down.

2.Reactor modeling

2.1. Hypotheses

The assumptions made in the present study for dynamic modeling and simulation of the reactor are as follows:

- Reactions occur in both bubble and emulsion phases.
- Radial concentration and temperature gradients in the reactor are negligible.
- Elutriation of solids at the top of the bed is neglected.
- Catalyst is fed continuously into the reactor as pre-polymer.
- Constant mean particle size is assumed throughout the bed.
- Overall movement of polymer particles is downward for both phases.

2.2.Kinetics

In this study, a comprehensive mechanism is considered to describe the copolymerization kinetics of ethylene and 1-butene over the Ziegler-Natta catalyst with two different active sites based on the kinetic model proposed by McAuley et al. [2]. The catalyst has multiple active sites leading to the production of polymers having broad, and often bimodal, molecular weight and copolymer composition distributions [6]. The key elementary reactions such as formation, initiation, propagation and chain transfer reactions are summarized in Table 1. The method of moments was used to model the polymer properties. The moment equations are shown in Table 2. Once the moment equations are solved, the rate of reaction for each component, assuming the monomers are mainly consumed through the propagation reactions, could be obtained from [2]:

$$R_i = \sum_{j=1}^{NS} [M_i] Y(0, j) kp_{Ti} \qquad i=1, 2 \qquad (1)$$

$$R_{H_2} = \sum_{j=1}^{NS} [M_i] Y(0, j) kfh_T \qquad (2)$$

where *NS* is the number of types of active sites. The kinetic rate constants were those proposed by Kiashemshaki et al. [9]. The polymer production rate R_p could be then calculated from:

$$R_p = \sum_{i=1}^{2} MW_i R_i + MW_{H_2} R_{H_2} \qquad (3)$$

in which R_i and R_{H_2} are the instantaneous rate of reaction for monomer *i* and hydrogen obtained from Eq. (1) and (2), respectively.

Table 1. Elementary reactions of ethylene polymerization system

Reaction	Description
$N^*(j) \xrightarrow{kf(j)} N(0, j)$	Formation reaction with co-catalyst
$N(0, j) + M_i \xrightarrow{ki_i(j)} N_i(1, j)$	Initiation reaction with monomers
$\mathrm{N_i(r, j) + M_i \xrightarrow{kp_{ik}(j)} N_i(r+1, j)}$	Propagation
$N_i(r, j) + M_i \xrightarrow{kfm_{ik}(j)} N_k(1, j) + Q(r, j)$	Transfer to monomer
$N_i(r, j) + H_2 \xrightarrow{kfh_i(j)} N_H(0, j) + Q(r, j)$ $N_H(0, j) + M_i \xrightarrow{kh_i(j)} N_i(1, j)$ $N_H(0, j) + AlEt_3 \xrightarrow{kh_r(j)} N_1(1, j)$	Transfer to hydrogen
$N_i(r, j) + AlEt_3 \xrightarrow{kfr_i(j)} N_1(1, j) + Q(r, j)$	Transfer to co-catalyst
$N_i(r, j) \xrightarrow{kfs_i(j)} N_H(0, j) + Q(r, j)$	Spontaneous transfer
$N_i(r, j) \xrightarrow{kds(j)} N_d(j) + Q(r, j)$ $N(0, j) \xrightarrow{kds(j)} N_d(j)$ $N_H(0, j) \xrightarrow{kds(j)} N_d(j)$	Deactivation reactions

Table 2. Moment equations

$\frac{dY(0,j)}{dt} = [M_T]\left\{ki_T(j)N(0,j) + kh_T(j)N_H(0,j)\right\} + kh_r(j)N_H(0,j)[AlEt_3] - Y(0,j)\left\{kfh_T(j)[H_2] + kfs_T(j) + kds(j) + \frac{R_v}{V_p}\right\}$
$\frac{dY(1,j)}{dt} = [M_T]\left\{ki_T(j)N(0,j) + kh_T(j)N_H(0,j)\right\} + kh_r(j)N_H(0,j)[AlEt_3] + [M_T]k_{P_{TT}}(j)Y(0,j) + \left\{Y(0,j) - Y(1,j)\right\} \left\{kfm_{TT}(j)[M_T] + kfr_T(j)[AlEt_3]\right\} - Y(1,j)\left\{kfh_T(j)[H_2] + kfs_T(j) + kds(j) + \frac{R_v}{V_p}\right\}$
$\frac{dY(2,j)}{dt} = [M_T]\left\{ki_T(j)N(0,j) + kh_T(j)N_H(0,j)\right\} + kh_r(j)N_H(0,j)[AlEt_3] + [M_T]kp_{TT}(j)\left\{2Y(1,j) - Y(0,j)\right\} + \left\{Y(0,j) - Y(2,j)\right\}\left\{kfm_{TT}(j)[M_T] + kfr_T(j)[AlEt_3]\right\} - Y(2,j)\left\{kfh_T(j)[H_2] + kfs_T(j) + kds(j) + \frac{R_v}{V_p}\right\}$
$\frac{dX(n,j)}{dt} = \left\{Y(n,j) - N_T(1,j)\right\}\left\{kfm_{TT}(j)[M_T] + kfr_T(j)[AlEt_3] + kfh_T(j)[H_2] + kfs_T(j) + kds(j)\right\} - X(n,j)\frac{R_v}{V_p} \qquad n = 0,1,2$

2.3. Hydrodynamics

Most researches have employed the simple two-phase concept for modeling the gas-phase ethylene polymerization (e.g., [3, 5, 6]). In the simple two-phase theory, it is assumed that all the gas in excess of that required for minimum fluidization passes through the bed as solid free bubbles while the emulsion stays at minimum fluidization conditions. Existence of solid particles in bubbles has been shown both experimentally [12, 13] and theoretically [14, 15]. The emulsion phase also does not remain at the minimum fluidization condition and may contain a higher amount of gas at higher gas velocity [13, 16]. Mostoufi et al. [17] showed that assuming the simple two-phase structure of the fluidized beds would result in under-predicting the performance of the reactor. They concluded that such an over-simplification of the flow structure of gas and solids in the fluidized bed reactors could be quite misleading in the prediction of the performance of such reactors. Based on these facts, the concentration of particles in both emulsion and bubble phases have been estimated in the present study from the dynamic two-phase concept of fluidization proposed by Cui et al. [11]. According to the dynamic two-phase concept of fluidization the bubbles may contain solid particles. In a real fluidized bed, the concentration of particles in the emulsion phase can be less than that at the minimum fluidization, and the bubbles can contain various amounts of particles [11, 18].

Adopting the concepts of the dynamic two-phase hydrodynamic structure [11], Jafari et

al. [10] proposed a sequential modular approach to modeling fluidized bed reactors. According to their procedure, a fluidized reactor should be divided into a number of serial sections in which each section consists of bubble and emulsion phases. The flow of gas is considered as plug flow through the bubbles and is perfectly mixed through the emulsion phase in each section. Number of sections is determined from Table 3 after evaluating the dimensionless number *J* (which includes both kinetic and hydrodynamic parameters) defined as:

$$J = Ha\frac{U_0}{U_{mf}} \tag{4}$$

Hata number in this reaction system could be determined from:

$$Ha = \frac{\left(D_g k_{Pik}(j) N_i(r,j)\right)^{0.5}}{K_{be}} \tag{5}$$

The accuracy of Jafari et al.'s model [10] has been confirmed by the experimental data reported in the literature over a wide range of superficial gas velocity.

Kiashemshaki et al. [9] adopted Jafari's model. [10] and developed it for a polyethylene fluidized reactor. They found that the number of sections in this case should be equal to four and showed that there is a good agreement between the model and actual polyethylene plant data. Therefore, the hydrodynamic model of Kiashemshaki et al. [9] has been employed in the present study. The schematic of such an arrangement is illustrated in Fig. 1. Equations used in this hydrodynamic model are also given in Table 4.

Table 3. Number of segments [10]

J	***N***
11.1 < *J*	1
5.62< *J* <11.1	2
0.63< *J* <5.62	3
J < 0.63	4

2.4. Mass balance equations

Based on the above hydrodynamic sub-model, dynamic molar balances for the two monomers (i.e., ethylene and 1-butene) and hydrogen in the *n*th section of the bed are given by the following equations:

Section 1:

Bubble:

$$[\mathrm{M_i}]_{\mathrm{b,(in)}}\mathrm{U_b A_b} - [\mathrm{M_i}]_{\mathrm{b,(1)}}\mathrm{U_b A_b} - \mathrm{F_{out}}\varepsilon_{\mathrm{b,(1)}}[\mathrm{M_i}]_{\mathrm{b,(1)}} - \mathrm{K_{be}V_{b,(1)}}([\mathrm{M_i}]_{\mathrm{b,(1)}} - [\mathrm{M_i}]_{\mathrm{e,(1)}}) - \frac{\mathrm{A_b}}{\mathrm{V_{PLUG,(1)}}}\int_{z_{(1)}}^{z_{(2)}}(\mathrm{R_{i_{b,(1)}}} + \mathrm{R_{H_{2b,(1)}}})\mathrm{V_{p_{b,(1)}}}\,\mathrm{dz} = \frac{\mathrm{d}}{\mathrm{dt}}\left(\mathrm{V_{b,(1)}}\varepsilon_{\mathrm{b,(1)}}[\mathrm{M_i}]_{\mathrm{b,(1)}}\right) \tag{6}$$

Emulsion:

$$[M_i]_{e,(in)}U_e A_e - [M_i]_{e,(1)}U_e A_e - F_{out}\varepsilon_{e,(1)}[M_i]_{e,(1)} + K_{be}V_{e,(1)}\left(\frac{\delta_{(1)}}{1-\delta_{(1)}}\right)([M_i]_{b,(1)} - [M_i]_{e,(1)}) - (R_{i_e} + R_{H_{2e}})_{(1)}V_{p_{e,(1)}} = \frac{d}{dt}\left(V_{e,(1)}\varepsilon_{e,(1)}[M_i]_{e,(1)}\right) \tag{7}$$

Table 4. Correlations and equations used in the hydrodynamic model

Parameter	Formula	Reference
Minimum fluidization velocity	$\mathrm{Re}_{mf} = \left[(29.5)^2 + 0.357Ar\right]^{1/2} - 29.5$	[19]
Bubble velocity	$U_b = U_0 - U_e + u_{br}$	[20]
Bubble rise velocity	$u_{br} = 0.711(gd_b)^{1/2}$	[20]
Emulsion velocity	$U_e = \dfrac{U_0 - \delta_{(n)}U_b}{1-\delta}$	
Bubble diameter	$d_b = d_{b0}\left[1+27(U_0-U_e)\right]^{1/3}(1+6.84h)$ d_{b0}=0.0085 for Geldart B	[21]
Mass transfer coefficient	$K_{be} = \left(\dfrac{1}{K_{bc}} + \dfrac{1}{K_{ce}}\right)^{-1}$ $K_{bc} = 4.5\left(\dfrac{U_e}{d_b}\right) + 5.85\left(\dfrac{D_g{}^{1/2} g^{1/4}}{d_b{}^{5/4}}\right)$ $K_{ce} = 6.77\left(\dfrac{D_g \varepsilon_{e,(n)} u_{br}}{d_b}\right)^{1/2}$	[22]
Heat transfer coefficient	$H_{be} = \left(\dfrac{1}{H_{bc}} + \dfrac{1}{H_{ce}}\right)^{-1}$ $H_{bc} = 4.5\left(\dfrac{U_e \rho_g C_{pg}}{d_b}\right) + 5.85\left(\dfrac{(k_g \rho_g C_{pg})^{1/2} g^{1/4}}{d_b{}^{5/4}}\right)$ $H_{ce} = 6.77(\rho_g C_{pg} k_g)^{1/2}\left(\dfrac{\varepsilon_{e,(n)} u_{br}}{d_b{}^3}\right)^{1/2}$	[23]
Bubble phase fraction	$\delta_{(n)} = 0.534\left[1 - \exp\left(-\dfrac{U_0 - U_{mf}}{0.413}\right)\right]$	[11]
Emulsion phase porosity	$\varepsilon_{e,(n)} = \varepsilon_{mf} + 0.2 - 0.059\exp\left(-\dfrac{U_0 - U_{mf}}{0.429}\right)$	[11]
Bubble phase porosity	$\varepsilon_{b,(n)} = 1 - 0.146\exp\left(-\dfrac{U_0 - U_{mf}}{4.439}\right)$	[11]
Volume of the emulsion phase in each section	$V_{e,(n)} = \dfrac{Ah(1-\delta_{(n)})}{4}$	
Volume of the bubble phase in each section	$V_{b,(n)} = \dfrac{Ah\delta_{(n)}}{4}$	
Volume of PFR in each section	$V_{PLUG,(n)} = V_{b,(n)}\varepsilon_{b,(n)}$	
Volume of polymer in the emulsion phase in each section	$V_{p_{e,(n)}} = \dfrac{Ah(1-\varepsilon_{e,(n)})(1-\delta_{(n)})}{4}$	
Volume of polymer in the bubble phase in each section	$V_{p_{b,(n)}} = \dfrac{Ah(1-\varepsilon_{b,(n)})\delta_{(n)}}{4}$	

Sections 2, 3, 4:
Bubble:

$$[M_i]_{b,(n-1)}U_bA_b-[M_i]_{b,(n)}U_bA_b-K_{be}V_{b,(n)}([M_i]_{b,(n)}-[M_i]_{e,(n)})-\frac{A_b}{V_{PLUG,(n)}}\int_{z_{(n-1)}}^{z_{(n)}}(R_{i_{b,(n)}}+R_{H_{2b,(n)}})V_{p_{b,(n)}}dz=$$
$$\frac{d}{dt}\left(V_{b,(n)}\varepsilon_{b,(n)}[M_i]_{b,(n)}\right) \quad (8)$$

Emulsion:

$$[M_i]_{e,(n-1)}U_eA_e-[M_i]_{e,(n)}U_eA_e+K_{be}V_{e,(n)}\left(\frac{\delta_{(n)}}{1-\delta_{(n)}}\right)([M_i]_{b,(n)}-[M_i]_{e,(n)})-$$
$$(R_{i_e}+R_{H_{2e}})_{(n)}V_{p_{e,(n)}}=\frac{d}{dt}\left(V_{e,(n)}\varepsilon_{e,(n)}[M_i]_{e,(n)}\right) \quad (9)$$

In the above equations, the direction of mass transfer is assumed to be from bubble to emulsion phase. It is worth noting that since the overall conversion in the polyethylene reactor is low (and in the bubbles is even lower), the concentration of the monomers in the bubble phase could be considered to be constant (or averaged) in each segment when calculating the accumulation terms.
The overall mass balance (equation of continuity) of the polymer in the bed, considering constant density and porosity, is:

$$\frac{1}{(1-\varepsilon_{ave})\rho_{pol}A}\left[F_{prepol}-F_{out}(1-\varepsilon_{ave})\rho_{pol}+Ah(1-\varepsilon_{ave})R_p\right]=\frac{dh}{dt} \quad (10)$$

where ε_{ave} should be evaluated from:

$$\varepsilon_{ave}=\delta\varepsilon_b+(1-\delta)\varepsilon_e \quad (11)$$

2.5. Energy balance equations
The energy balance equations are:

Section 1:
Bubble:

$$\begin{aligned}
&U_bA_b(T_{b,(in)}-T_{ref})\sum_{i=1}^{4}C_{p_i}[M_i]_{b,(in)}-U_bA_b(T_{b,(1)}-T_{ref})\sum_{i=1}^{4}C_{p_i}[M_i]_{b,(1)}\\
&+\sum_{n=2}^{4}(R_{p_{b,(n)}})_{b,(2)}C_{p,pol}(T_{b,(2)}-T_{ref})\\
&-F_{out}(T_{b,(1)}-T_{ref})\left(\varepsilon_{b,(1)}\sum_{i=1}^{4}C_{p_i}[M_i]_{b,(1)}+(1-\varepsilon_{b,(1)})\rho_{pol}C_{p.pol}\right)\\
&+\Delta H_R\frac{A_b}{V_{PLUG,(1)}}\left(\sum_{i=1}^{2}\int_{z(1)}^{z(2)}R_{i_{b,(1)}}V_{p_{b,(1)}}dz+\int_{z(1)}^{z(2)}R_{H_{2b,(1)}}V_{p_{b,(1)}}dz\right)\\
&+H_{be}V_{b,(1)}(T_{e,(1)}-T_{b,(1)})\\
&=\frac{d}{dt}\left(V_{b,(1)}(T_{b,(1)}-T_{ref})\left[\varepsilon_{b,(1)}\sum_{i=1}^{4}C_{p_i}[M_i]_{b,(1)}+(1-\varepsilon_{b,(1)})\rho_{pol}C_{p,pol}\right]\right)
\end{aligned} \quad (12)$$

Emulsion:

$$
\begin{aligned}
&U_e A_e (T_{e,(in)} - T_{ref}) \sum_{i=1}^{4} C_{p_i} [M_i]_{e,(in)} - U_e A_e (T_{e,(1)} - T_{ref}) \sum_{i=1}^{4} C_{p_i} [M_i]_{e,(1)} \\
&+ \sum_{n=2}^{4} (R_{p_{e,(n)}})_{e,(2)} C_{p,pol} (T_{e,(2)} - T_{ref}) - \\
&- F_{out} (T_{e,(1)} - T_{ref}) \left(\varepsilon_{e,(1)} \sum_{i=1}^{4} C_{p_i} [M_i]_{e,(1)} + (1 - \varepsilon_{e,(1)}) \rho_{pol} C_{p,pol} \right) \\
&+ \Delta H_R \left(\sum_{i=1}^{2} (R_{i_{e,(1)}} V_{p_{e,(1)}}) + R_{H_{2e,(1)}} V_{p_{e,(1)}} \right) - H_{be} V_{e,(1)} \left(\frac{\delta_{(1)}}{1 - \delta_{(1)}} \right) (T_{e,(1)} - T_{b,(1)}) \\
&= \frac{d}{dt} \left(V_{e,(1)} (T_{e,(1)} - T_{ref}) \left[\varepsilon_{e,(1)} \sum_{i=1}^{4} C_{p_i} [M_i]_{e,(1)} + (1 - \varepsilon_{e,(1)}) \rho_{pol} C_{p,pol} \right] \right)
\end{aligned}
\tag{13}
$$

Sections 2, 3, 4:
Bubble:

$$
\begin{aligned}
&U_b A_b (T_{b,(n-1)} - T_{ref}) \sum_{i=1}^{4} C_{p_i} [M_i]_{b,(n-1)} - U_b A_b (T_{b,(n)} - T_{ref}) \sum_{i=1}^{4} C_{p_i} [M_i]_{b,(n)} \\
&+ \left(\sum_{n+1}^{4} (R_{p_{b,(n)}})_{b,(n+1)} \right) C_{p,pol} (T_{b,(n+1)} - T_{ref}) - \left(\sum_{n}^{4} (R_{p_{b,(n)}})_{b,(n)} \right) C_{p,pol} (T_{b,(n)} - T_{ref}) \\
&+ \Delta H_R \frac{A_b}{V_{PLUG,(n)}} \left(\sum_{i=1}^{2} \int_{z(n-1)}^{z(n)} R_{i_{b,(n)}} V_{p_{b,(n)}} dz + \int_{z(n-1)}^{z(n)} R_{H_{2b,(n)}} V_{p_{b,(n)}} dz \right) \\
&+ H_{be} V_{b,(n)} (T_{e,(n)} - T_{b,(n)}) \\
&= \frac{d}{dt} \left(V_{b,(n)} (T_{b,(n)} - T_{ref}) \left[\varepsilon_{b,(n)} \sum_{i=1}^{4} C_{p_i} [M_i]_{b,(n)} + (1 - \varepsilon_{b,(n)}) \rho_{pol} C_{p,pol} \right] \right)
\end{aligned}
\tag{14}
$$

Emulsion:

$$
\begin{aligned}
&U_e A_e (T_{e,(n-1)} - T_{ref}) \sum_{i=1}^{4} C_{p_i} [M_i]_{e,(n-1)} - U_e A_e (T_{e,(n)} - T_{ref}) \sum_{i=1}^{4} C_{p_i} [M_i]_{e,(n)} \\
&+ \left(\sum_{n+1}^{4} (R_{p_{e,(n)}})_{e,(n+1)} \right) C_{p,pol} (T_{e,(n+1)} - T_{ref}) - \left(\sum_{n}^{4} (R_{p_{e,(n)}})_{e,(n)} \right) C_{p,pol} (T_{e,(n)} - T_{ref}) \\
&+ \Delta H_R \left(\sum_{i=1}^{2} (R_{i_{e,(n)}} V_{p_{e,(n)}}) + R_{H_{2e,(n)}} V_{p_{e,(n)}} \right) - H_{be} V_{e,(n)} \left(\frac{\delta_{(n)}}{1 - \delta_{(n)}} \right) (T_{e,(n)} - T_{b,(n)}) \\
&= \frac{d}{dt} \left(V_{e,(n)} (T_{e,(n)} - T_{ref}) \left[\varepsilon_{e,(n)} \sum_{i=1}^{4} C_{p_i} [M_i]_{e,(n)} + (1 - \varepsilon_{e,(n)}) \rho_{pol} C_{p,pol} \right] \right)
\end{aligned}
\tag{15}
$$

Note that the overall direction of movement of polymer particles in the bed is the opposite of that for the gaseous stream (see Fig. 1).

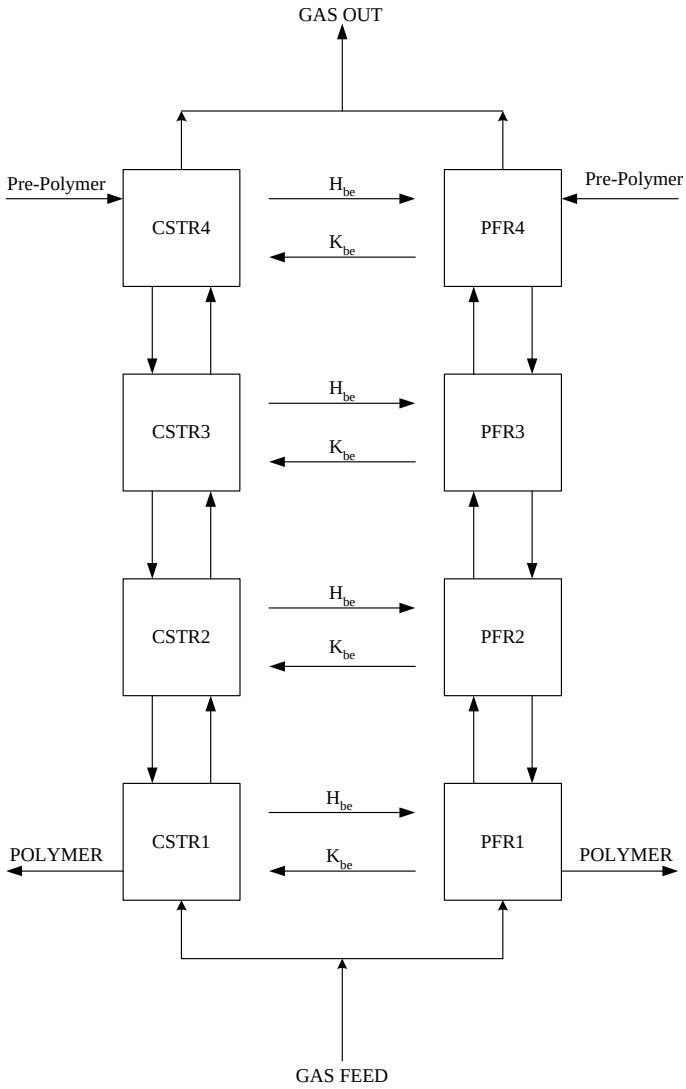

Figure 1. Schematic diagram of the modeling structure of fluidized bed

Once the energy balance equations are solved, the temperature of the unreacted gases exit from the top of the reactor could be evaluated from:

$$T_{ave} = \frac{C_{p_b}\delta T_b + C_{p_e}(1-\delta)T_e}{C_{p_b}\delta + C_{p_e}(1-\delta)} \qquad (16)$$

where C_{p_b} and C_{p_e} are the molar averaged specific heat capacity of the gas in bubble and emulsion phases in the outlet gaseous stream from the top of the reactor, respectively.

2.6. Level controller

Level of the solids in the bed is controlled by the volumetric rate of the product withdrawn

from the reactor. A proportional-integral-derivative (PID) controller has been used for this purpose. The general control equation describing the PID controller is given by:

$$OP(t) = K_c E(t) + \frac{1}{\tau_i}\int_0^t E(t)dt + \tau_d \frac{dE(t)}{dt} \qquad (17)$$

The tuned controller parameters are given in Table 5.

Table 5. Parameters of the controller

Parameter	Value
K_c	-0.08
$\frac{1}{\tau_i}$	-0.00001
τ_d	-17

2.7. Polymer molecular weight

In order to evaluate the molecular weight of the polymer produced in the reactor at any time, dynamic molar balances have been developed for the number of moles of the two monomers incorporated or bounded inside the polymer particles of each phase:

Section 1:

$$n_{i,(2)}\frac{R_{v,(2)}}{V_{p,(2)}} - \frac{n_{i,(1)}F_{out}(1-\varepsilon_{(n)})}{V_{p,(1)}} + R_{i,(1)}V_{p,(1)} = \frac{dn_{i,(1)}}{dt} \qquad (18)$$

Sections 2, 3, 4:

$$n_{i,(n+1)}\frac{R_{v,(n+1)}}{V_{p,(n+1)}} - n_{i,(n)}\frac{R_{v,(n)}}{V_{p,(n)}} + R_{i,(n)}V_{p,(n)} = \frac{dn_{i,(n)}}{dt} \qquad (19)$$

The weight average molecular weights of the polymer could be then evaluated from:

$$\overline{M}_w = \frac{\overline{m}\sum_{j=1}^{NS}\{X(2,j)+Y(2,j)\}}{\sum_{j=1}^{NS}\{X(1,j)+Y(1,j)\}} \qquad (20)$$

3. Results and discussion

The proposed model is comprised of 145 ordinary differential equations (ODE). There are 18 equations for each phase of the reactor including 3 molar balance equations for the monomers and hydrogen, one energy balance equation, 2 molar balance equations for the monomers incorporated or bounded in the polymer particles and 12 moment equations. The equation of the level controller is also added to the above set of equations. These equations were solved for start-up at the operating conditions given in Table 6. These operating conditions and the related plant data were gathered from the polyethylene plant of Arak Petrochemical Complex. The catalyst injection rate was adjusted such that the desired value of the polymer production rate at the outlet would be reached.

Table 6. Operating conditions of the reactor

Parameter	Unit	Value
h (initial)	m	8
h (set point)	m	11
D_t	m	3.9
U_0	m/s	0.57
T_{in}	K	317
P	bar(g)	19
d_p	μm	1145
Ethylene	%	40
1-Butene	%	17
Hydrogen	%	9
Inert gas	%	34

A comparison between results of the simulation and the actual plant data for a sample grade of LLDPE is given in Table 7. As shown in the table, there is a good agreement between operating conditions (temperature and production rate) predicted by the model and the real plant data. Actual weight average molecular weights reported in Table 7 were estimated based on the measured melt flow index of the product [9]. Calculated average molecular weights are also close to the real molecular weights.

Evolution of the bed height vs. time at the specified operating conditions is illustrated in Fig. 2. It can be seen in this figure that the bed height has reached the set point after about 8 hours and remained stable afterwards. Peaks (or valleys) in the bed height would have a considerable effect on the performance of the reactor because it determines the residence time of solids and the gas in the reactor. This effect is shown and discussed in the following figures.

Table 7. Comparison between the simulation results and the experimental data

Time after start -up (hr)	Temperature (°C)		Production Rate (ton/hr)		Average Molecular Weight (kg/kgmol)	
	Actual plant data	Simulation results	Actual plant data	Simulation results	Actual plant data	Simulation results
6	100.0	96.9	-	-	1.10×10^5	1.00×10^5
14	93.6	92.2	-	-	1.18×10^5	1.03×10^5
22	90.0	92.0	8.9	8.6	1.15×10^5	1.02×10^5

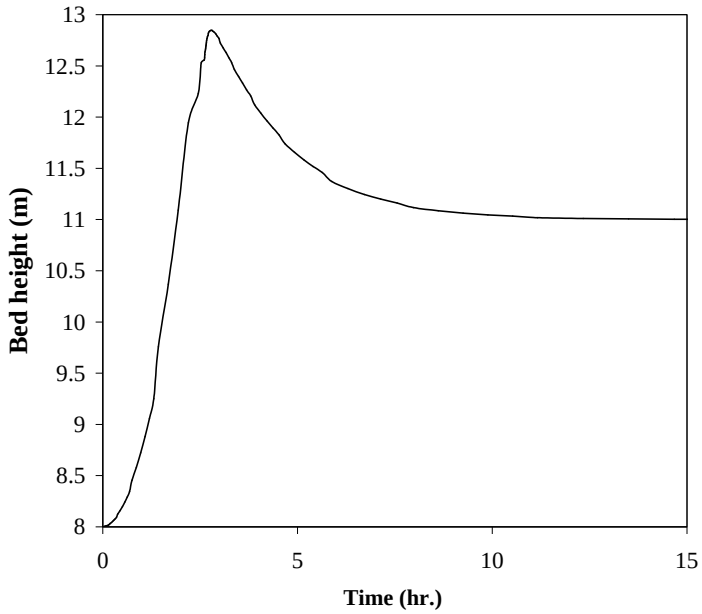

Figure 2. Bed height vs. time of operation

The outlet mole percent of ethylene in the bubble and emulsion phases are shown in Fig. 3. As expected, the concentration of ethylene in the bubble phase is higher than that in the emulsion phase due to the lower amount of particles in the bubble phase. It is also seen in this figure that ethylene in the emulsion phase is consumed faster (higher slope of the curve) than in the bubble phase. The minima in the concentrations are due to the occurrence of a maximum in the bed height since the maximum height of the bed results in the maximum residence time of the reactants in the bed. Monomers are consumptions that are proportional to the residence time of the gas, thus, monomer concentrations reduce when the height of the bed increases.

Fig. 4 illustrates the rate of production of polymer in the reactor, as well as in the bubbles and emulsion phase, as a function of time of operation. As could be seen in this figure, maximum production occurs when the bed height reaches its maximum (see Fig. 2). As mentioned above, the reason for reaching a maximum of production at the same time that the bed height becomes maximum is that the residence time of monomer gases in the bed is proportional to the bed height. As a result, more polymers would be produced when the bed height is increased.

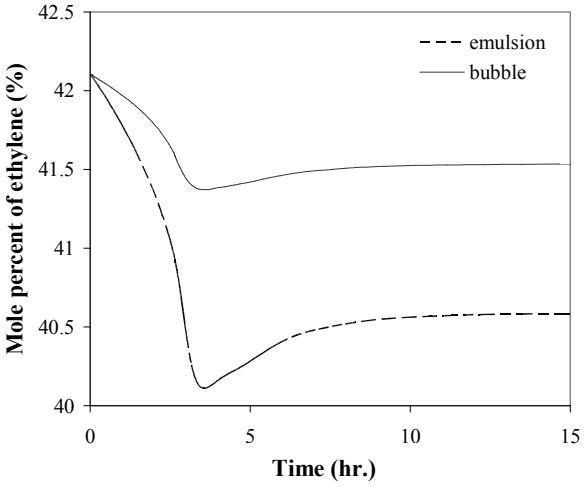

Figure 3. Mole percent of ethylene in the bubble and emulsion phases

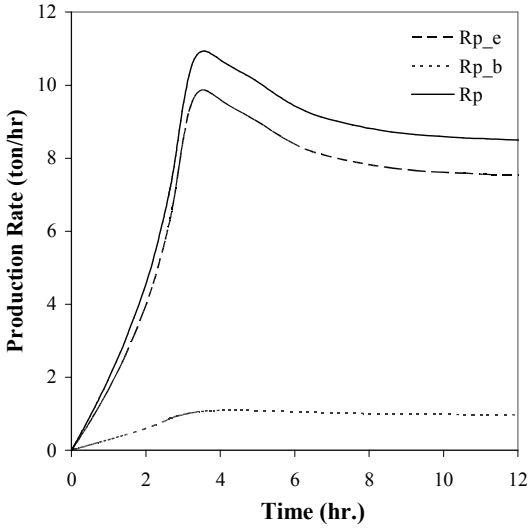

Figure 4. Production rate of the polymer vs. time of operation

Moreover, it can be seen in Fig. 4 that the production rate of polymer in the bubble phase is less than that in the emulsion phase due to the fact that emulsion contains more catalyst. It could be concluded from Fig. 4 that about 88% of the product is produced in the emulsion phase while the share of the bubbles in the production is around 12%. It is worth mentioning that the catalyst is distributed among this phase in almost the same portion. Fig. 4 confirms that contribution of solid particles inside the bubble phase is not negligible in production of the polymer, as previously pointed out by Kiashemshaki et al. [9].

The difference between the temperatures of the bubble and emulsion phases is illustrated in Fig. 5. As expected, the emulsion phase temperature is significantly higher than the bubble phase temperature because of the higher polymer production rate in the emulsion phase. Occurrence of the maximum in the temperature corresponds to the maximum in the bed height, as discussed above.

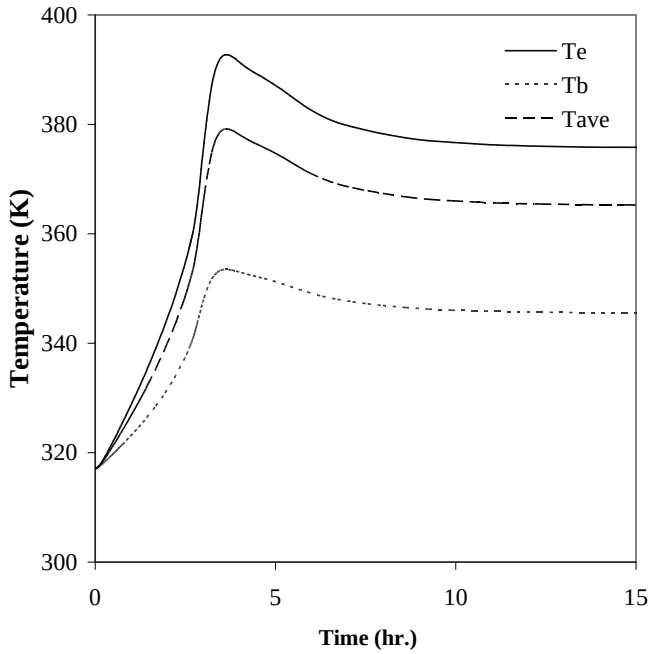

Figure 5. Bubble and emulsion phase temperatures

Control of gas-phase polymerization reactors is a complicated task because of the high non-linearity of the system. In an industrial gas-phase polyethylene reactor, controlling the bed level is one of the most critical and difficult tasks. It has been shown in the previous figures that all the process values in the bed are correlated to the height of the solids in the reactor. It is known that when a large process is to be controlled, the proportional controller is suitable. This is the case for many liquid level control loops. Also, the effect of proportional gain is more significant than the integral and derivative time. Therefore, the effect of K_c on the reactor was investigated after setting integral and derivative terms into their reasonable values. The trend illustrated in Fig. 2 has

been achieved after tuning the control parameters in order to damp the level fluctuations and reach the desired value. It is important to mention that an improper tuning of the level controller would result in an oscillation pattern, loosening the bed or increasing the bed height without a practical limit. Sensitivity of the solids level in the reactor with the parameters of the controller is illustrated in Fig. 6. Sensitivity of the bed behavior to the value of the proportional gain of the controller is shown in this figure while other parameters of the controller are kept unchanged. It is shown that in this case, the level of the bed could be properly controlled when K_c is less than -0.25. This figure shows that selecting an improper gain might lead to loosening the control of the level of the bed. It is then necessary to further investigate the dynamic behavior of the bed more thoroughly and carryout dynamic optimization of the polyethylene reactor at different unsteady-state conditions.

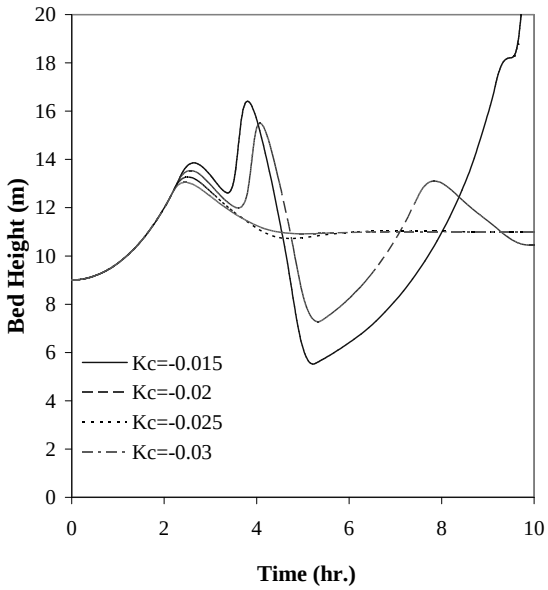

Figure 6. Variation of the level of the bed vs. time of operation at different proportional gains

4. Conclusions

A two-phase model consisting of 145 ODEs has been developed to predict the dynamic behavior of the gas phase fluidized bed reactor of ethylene polymerization. The reactor was divided into four serial sections where each section consists of bubble and emulsion phases. Flow of the gas was considered as plug flow through the bubbles and perfectly mixed through the emulsion phase. Existence of solids in the bubbles was considered in the present study, thus, the polymerization reactions occur in both emulsion and bubble phases. Dynamic simulation of the reactor was accomplished by means of integrating the model equations along with controlling the bed height with a PID controller.Due to high non-linearity of the model equations, controlling the gas-phase polymerization reactor is a difficult task. Controlling the bed height is an important factor in the reactor performance. It was shown that peaks or valleys of the bed height have a significant effect on all of the

reactor variables, especially those related to the emulsion phase due to a higher contribution of this phase in the production rate. Results of the simulation were compared with the plant data and a close agreement was observed between the model prediction and real data. It has been shown that since there is a significant amount of catalyst particles in the bubble phase, neglecting the production rate in this phase could lead to significant error. The proposed model is suitable for simulating the dynamic behavior of the reactor at start-up, shut-down and grade transition.

Acknowledgements
The authors gratefully acknowledge all the help from Mr. A. Kiashemshaki. The authors would also like to thank Mr. S. Mostafavi from Arak Petrochemical Complex for his comments and providing useful information in different stages of the study.

Notation

A cross sectional area of the reactor, m^2
$AlEt_3$ triethyl aluminum
Ar Archimedes number
C_{p_i} specific heat capacity of component i, J/kg.K
$C_{p,pol}$ specific heat capacity of solid product, J/kg.K
d_b bubble diameter, m
d_p particle diameter, m
D_g gas diffusion coefficient, m^2/s
D_t reactor diameter, m
E deviation from set point
F_{out} volumetric product removal rate, m^3/s
F_{prepol} pre-polymer flow rate, kg/s
k_g gas thermal conductivity, W/m.K
J dimensionless no.
kfh_i transfer to hydrogen rate constant for a polymer chain with terminal monomer i, m^3/kmol.s
kfm_{ik} transfer to monomer k rate constant for a polymer chain with terminal monomer i, m^3/kmol.s
kfr_i transfer to co-catalyst rate constant for a polymer chain with terminal monomer i, m^3/kmol.s
kfs_i spontaneous transfer rate constant for a polymer chain with terminal monomer i, m^3/kmol.s
kh_i rate constant for re-initiation by monomer i, m^3/kmol.s
kh_r rate constant for re-initiation by co-catalyst i, m^3/kmol.s
ki_i rate constant for initiation by monomer i, m^3/kmol.s
kp_{ik} propagation rate constant for a polymer chain with terminal monomer i reacting with monomer k,m^3/kmol.s
K_{bc} bubble to cloud mass transfer coefficient, s^{-1}
K_{be} bubble to emulsion mass transfer coefficient, s^{-1}
K_c proportional gain of the controller
K_{ce} cloud to emulsion mass transfer coefficient, s^{-1}
Kds spontaneous deactivation rate constant, s^{-1}
Kf Formation rate constant, s^{-1}
h bed height, m
Ha Hata number
H_{bc} bubble to cloud heat transfer coefficient, $W/m^3.K$
H_{ce} cloud to emulsion heat transfer coefficient, $W/m^3.K$
H_{be} bubble to emulsion heat transfer coefficient, $W/m^3.K$
m number of monomers
$\overline{m}$ mean monomer molecular weight, kg/kgmol
$[M_i]$ concentration of component i in the reactor, $kmol/m^3$
$[M_i]_{in}$ concentration of component i in the inlet gaseous stream
$[M_T]$ total molar monomer concentration, $kmol/m^3$
M_i the ith monomer
$\overline{Mw}$ weight average molecular weight, kg/kmol
MW_i molecular weight of monomer i, kg/kmol

MW_{H_2} molecular weight of hydrogen, kg/kmol
$N(0,j)$ active site type j produced by formation reaction
$N^*(j)$ potential active site type j
$N_d(j)$ spontaneously deactivated site of type j
$N_H(0,j)$ active site of type j produced by transfer to hydrogen
$N_i(r,j)$ live polymer of length r growing on site of type j with terminal monomer i
NS number of type of active sites
n_i number of moles of reacted monomer i bound in the polymer in the reactor, kmol
OP controller output
P pressure, Pa
$Q(r,j)$ dead polymer of length r produced at site of type j
R_{i_b} instantaneous rate of reaction for monomer i in the bubble phase, kmol/m^3.s
R_{i_e} instantaneous rate of reaction for monomer i in the emulsion phase, kmol/m^3.s
R_i instantaneous rate of reaction for monomer i, kmol/m^3.s
R_{H_2} instantaneous rate of reaction for hydrogen, kmol/m^3.s
R_p production rate, kg/m^3.s
R_v volumetric flow rate of polymer from the reactor, m^3/s
t operating time, s
T temperature, K
T_{in} temperature of the inlet gaseous stream , K
U_0 superficial gas velocity, m/s
U_b bubble velocity, m/s
U_e emulsion gas velocity, m/s
U_{mf} minimum fluidization velocity, m/s
V volume, m^3
V_{PLUG} volume of PFR in each section, m^3
V_p volume of polymer inside the reactor, m^3
$X(n,j)$ nth moment of dead polymer produced at site of type j
$Y(n,j)$ nth moment of live polymer produced at site of type j
z axial position, m

Greek letters

ΔH_R heat of reaction, KJ/kmol
δ volume fraction of bubbles in bed
ε void fraction
ε_{ave} average voidage of the bed
μ gas viscosity, Pa.s
ρ density, kg/m^3
τ_i integral time, s
τ_d derivative time, s

Subscripts and superscripts

1 ethylene
2 1-butene
3 hydrogen
4 inert gas
b bubble phase
e emulsion phase
g Gas
in feed or inlet
i monomer type no.
j active site type no.
mf minimum fluidization
n section no.
pol polymer
ref reference conditions

References

1. Choi, K. Y., Ray, W. H., "The dynamic behaviour of fluidized bed reactors for solid catalysed gas phase olefin polymerization", *Chem. Eng. Sci.*, 40, 2261-2279 (1985).
2. McAuley, K. B., Macgregor, J. F., Hamielec, A. E., "A kinetic model for industrial gas-phase ethylene copolymerization", *AIChE J.*, 36, 837-850 (1990).
3. McAuley, K. B., Talbot, J. P., Harris, T. J., "A comparision of two phase and well-mixed models for fluidized bed polyethylene reactors", *Chem. Eng. Sci.*, 49, 2035-2045 (1994).
4. Fernandes, F. A. N., Lona, L. M. F., "Fluidized bed reactor and physical-chemical properties modeling for

polyethylene production", *Comp. Chem. Eng.*, 23, S803- S806 (1999).
5. Fernandes, F. A. N., Lona, L. M. F., "Heterogeneous modeling for fluidized bed polymerization reactor", *Chem. Eng. Sci.*, 56, 963-969 (2001).
6. Hatzantonis, H., Yiannoulakis, H., Yiagopoulos, A., Kiparissides, C., "Recent developments in modeling gas-phase catalyzed olefin polymerization fluidized-bed reactors: The effect of bubble size variation on the reactor's performance", *Chem. Eng. Sci.*, 55, 3237-3259 (2000).
7. Chatzidoukas, C., Perkins, J. D., Pistikopoulos, E. N., Kiparssides, C. "Optimal grade transition and selection of closed-loop controllers in a gas-phase olefin polymerization fluidized bed reactor", *Chem. Eng. Sci.*, 58, 3643-3658, (2003).
8. Alizadeh, M., Mostoufi, N., Pourmahdians, S., Sotudeh-Gharebagh, R., "Modeling of fluidized bed reactor of ethylene polymerization", *Chem. Eng. J.*, 97, 27-35 (2004).
9. Kiashemshaki, A., Mostoufi, M., Sotudeh-Gharebagh, R., "Two-phase modeling of the gas phase polyethylene fluidized bed reactor", Chem. Eng. Sci., 61, 3997-4006 (2006).
10. Jafari, R., Sotudeh-Gharebagh, R., Mostoufi, N., "Modular simulation of fluidized bed reactors", *Chem. Eng. Technol.*, 27, 123-122, Erratum (2004), 27, 224 (2004).
11. Cui, H., Mostoufi, N., Chaouki, J., "Characterization of dynamic gas-solid distribution in fluidized beds", *Chem. Eng. J.*, 79, 133-143 (2000).
12. Aoyagi, M., Kunni, D., "Importance of dispersed solids in bubbles for exothermic reactions in fluidized beds". *Chem. Eng. Commun.*, 1, 191-197 (1974).
13. Chaouki, J., Gonzalez, A., Guy, C., Klvana, D., "Two-phase model for a catalytic turbulent fluidized-bed reactor: Application to ethylene synthesis", *Chem. Eng. Sci.*, 54, 2039-2045 (1999).
14. Batchelor, G. K., Nitche, J. M., "Expulsion of particles from a buoyant blob in a fluidized bed", *J. Fluid Mech.*, 278, 63-81 (1994).
15. Gilbertson, M. A., Yates, J. G., "The motion of particles near a bubble in a gas-fluidized bed", *J. Fluid Mech.*, 323, 377-385 (1996).
16. Abrahamson, A. R., Geldart, D., "Behaviour of gas-fluidized beds of fine powders: Part II, Voidage of the dense phase in bubbling beds", *Powder Technol.*, 26, 47-55 (1980).
17. Mostoufi, N., Cui, H., Chaouki, J., "A comparison of two- and single-phase models for fluidized bed reactors", *Ind. Eng. Chem. Res.*, 40, 5526-5532 (2001).
18. Li, J. H., Wen, L. X., Qian, G. H., Cui, H. P., Kwauk, M., Schouten, J. C., van den Bleek, C. M., "Structure heterogeneity, regime multiplicity and nonlinear behavior in particle-fluid systems", *Chem. Eng. Sci.*, 51, 2693-2698 (1996).
19. Lucas, A., Arnaldos, J., Casal, J., Puigjaner, L., "Improved equation for the calculation of minimum fluidization velocity", *Ind. Eng. Chem. Proc. Des. Develop.*, 25, 426-429 (1986).
20. Davidson, J. F., Harrison, D., *Fluidized Particles*, Cambridge University Press, New York (1963).
21. Hilligardt, K., Werther, J., "Local bubble gas hold-up and expansion of gas/solid fluidized beds", *Ger. Chem. Eng.*, 9, 215-221 (1986).
22. Kunni, D., Levenspiel, O. *Fluidization Engineering*, 2nd ed., Boston, MA, Butterworth-Heinmann (1991).